Universitat Politècnica de Catalunya (UPC)
Universitat Autònoma de Barcelona (UAB)
Universitat de Barcelona (UB)
Institut de Ciències Fotòniques (ICFO)

http://www.photonicsbcn.eu

Master in Photonics

MASTER THESIS WORK

An experimental setup for gray molasses sub-Doppler cooling of potassium gases

Manel Bosch Aguilera

Supervised by Dr. Leticia Tarruell, (ICFO)

Presented on date 9th September 2014

Registered at

Escola Tècnica Superior d'Enginyeria de Telecomunicació de Barcelona

An experimental setup for gray molasses sub-Doppler cooling of potassium gases

Manel Bosch Aguilera

ICFO-Institut de Ciències Fotòniques, Parc Mediterrani de la Tecnologia, 08860 Barcelona, Spain

E-mail: manel.bosch@icfo.es

Abstract. An experimental setup for cooling a gas of potassium atoms below the Doppler limit is presented. This method is known as gray molasses cooling. It will be implemented using light blue detuned with respect to the the D_1 transition of potassium.

Keywords: ultracold quantum gases, laser cooling, sub-Doppler cooling, gray molasses.

1. Introduction

During the past decade and a half, quantum simulation with systems of ultracold quantum gases has proven to be a very effective tools for studying manybody physics [1]. On the one hand, this is due to the universality of Quantum Mechanics, that allows us to simulate a given system S by means of another one with different constituents S' as long as they share an equivalent Hamiltonian H. On the other hand, the value of this systems for quantum simulation lies in the fact that light-matter interaction and ultracold quantum gases are both nowadays well known fields. One of the biggest strenghts of such systems is the high precision one has to control all the parameters of the experiment. Moreover, the fact that this systems are dilute as opposed to those found in condensed matter (e.g. liquid helium) makes their description considerably simpler.

A celebrated example is the optical latice [2], in which the lattice seen by the electrons of a real solid, i.e., the *crystal* generated by the atomic cores, is substituted by the periodical potential created by non-resonant standing waves. The role of the electrons is now played by ultracold atoms. This allows the study of a broad range of solid state physics phenomena.

Other examples [3] might involve the generation of artificial gauge fields and also, thanks to the use of magetic fields, by mean of the so-called Fesbach resonances, it is possible to tune the particle-particle interactions; which opens the door to study manybody strongly correlated systems.

The group in which this project has been done is nowadays building a new experiment. This experiment is designed to use as atomic species the three isotopes of potassium: ^{39}K and ^{41}K, bosons, and ^{40}K. a fermion. This, together with the fact that potassium has broad Feshbach resonances at accessible magnetic fields for Bose gases, Fermi-Bose and Fermi-Fermi mixtures, makes potassium a unique atom and will allow us to work with either fermionic or bosonic strongly correlated gases and also mixtures of them. For instance, we will be able to study polaron physics (e.g. fermionic impurities in a bosonic bath or viceversa) and, in the long run, generate tunable optical lattices for fermions in order to study quantum magnetism and quantum phase transitions.

The first step in all this kind of experiments is to obtain what is known as a degenerate (fermionic or bosonic) quantum gas, i.e., a gas of particles whose properties are determined by

quantum mechanical effects. For this, it is necessary to cool down the atoms to a point in which their de Broglie wavelength becomes comparable to the interparticle distance so that the wave functions of the particles overlap. This point is reached when the phase space density is greater or equal than 1.

Reaching quantum degeneracy involves two techniques nowadays standard: laser cooling followed by evaporative cooling. However, due to the closely spaced hyperfine structure of its D_2-line (where alkali cooling is usually performed) standard sub-Doppler cooling techniques are hard to implement, which limits the minimum temperature achievable through laser cooling. To overcome this and improve the conditions for starting evaporative cooling, another method known as gray molasses cooling [4, 5, 6] should allow us to laser cool below the Doppler limit. The work done during this project has consisted on building the laser system responsible of this sub-Doppler cooling stage.

This report is organised as follows: in Sec. 2 our experimental setup is presented and we give an explanation of the cooling steps that will be implemented. In Sec. 3 the cooling process involved in gray molasses is presented. Finally, in Sec. 4 the laser system used for gray molasses cooling is explained in detail.

2. Experimental setup

As mentioned before, in order to obtain a degenerate quantum gas, an initial vapour of the atomic species of interest (potassium in our case) needs to be cooled down. For this, it is necessary a laser system that generates light at right frequencies and powers and a vacuum system into which this light will be sent to and where the cooling stages will take place.

The laser system has been designed in such a way that will allow us to cool any of the potassium isotopes and even mixtures of them. The transitions used for both cooling and repumping are shown in figure 2.

Our vacuum system is shown in figure 1. First of all, an ampoule containing an enriched sample of the isotope of our interest will be broken inside one of the bellows (1). Thanks to a temperature gradient, this vapour will arrive to a $2D^+$ magneto-optical trap [8] ($2D^+$-MOT) (3) which will be maintained at a pressure of $\sim 10^{-7}$ mbar thanks to an ion pump (2).

The purpose of this chamber is to produce a cold atomic beam. For this, the atoms will undergo a first laser cooling stage involving Doppler cooling [7] on the D_2-line in presence of a 2D quandrupole magnetic field created by permanent magnets, resulting in a transversely cooled atomic beam which will be pushed by a laser beam to the next chamber †.

The atoms will be then transported through the differential pumping tube (4) to the science chamber (6), maintained at ultra-high vacuum ($\sim 10^{-12}$ mbar) by the non evaporative getter and ion pumps (7). Here, a 3D-MOT will be implemented by sending six red detuned counter propagating beams. A 3D quadrupole magnetic field will be created a pair of Bitter coils (5) in anti-Helmholtz configuration. After this, the magnetic field will be turned off and additional molasses cooling will be performed. We expect to get in this stage some sub-Doppler cooling. However, for the reasons stated before, sub-Doppler cooling in the D_2-line of potassium is highly inefficient and a stage involving sub-Doppler cooling on the D_1-line (gray molasses) will be performed.

The final step is to transfer the atoms to a hybrid trap [10], formed by a quadrupole magnetic trap and an dipole trap (created by a Nd:YAG at 1064 nm). Here we will perform evaporative

† In the $2D^+$-MOT configuration, longitudinal molasses cooling is achieved using a counterpropagating beam sent through an in-vacuum 45° mirror

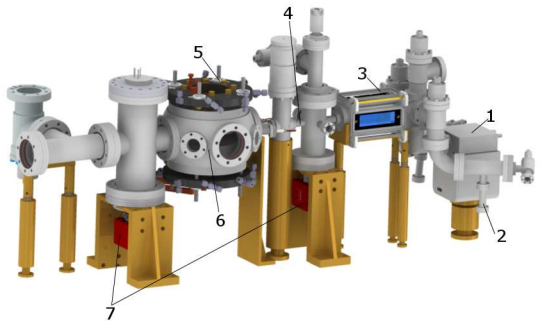

Figure 1. Vacuum system. 1. Ion pump 2. Bellow to load the species 3. $2D^+$-MOT with permanent magnets 4. Differential pumping tube 5. Bitter coil 6. Science Chamber 7. Non Evaporative Getter and Ion pumps.

cooling, where by using radio-frequency transitions, the most energetic atoms will be selectively expelled from the trap. This process will be repeated until reaching quantum degenerancy.

3. Gray molasses sub-Doppler cooling

3.1. Motivation.

As stated in the previous section, the hyperfine structure of the D_2 energy manifold is very narrow (c.f. figure 2). We can see that the energy splitting the $m_{F'}$ sublevels are of the order of the natural linewidth $\Gamma = 2\pi \times 6.03$ MHz. This leads to off-resonant excitation from the $F = 2 \to F' = 2$ for the bosonic isotopes or $F = 9/2 \to F' = 9/2$ for the fermionic one. This means that it is hard to isolate one single cooling transition. On the one hand, this implies that the role of the repumper beam will be important and therefore its power needs to be also high†. On the other hand, what happens is that we are effectively increasing the linewidth of the excited state. Consequently, the minimum Doppler temperature is also increased. To circumvent this difficulty we will apply a different cooling scheme known as gray molasses cooling.

Therefore, a first reason to use the D_1-line is that its states are much more separated and off-resonant transitions should be less important. Moreover, as we will see, the transitions involved can give rise to states that are not coupled to light, leading to a more efficient cooling.

3.2. Cooling mechanism

We will present here a toy model describing the cooling mechanism known as Gray Molasses [12]. One of the key points of these mechanism is the fact that, for $F \to F' = F$ or $F \to F' = F - 1$ transitions, there is at least one state which is not coupled to the laser field, whatever its polarization (as opposed to what happens with the usual transitions $F \to F' = F+1$ used for standard molasses). As a simple example, let us consider an $F = 1 \to F' = 1$ transition: we can see (figure 3(a) (up)) that, due to angular momentum conservation, a σ_+-polarized (resp. σ_-) beam cannot excite the $|g_{+1}\rangle$ (resp. $|g_{-1}\rangle$) state, and that a π-polarized one cannot excite the $|g_0\rangle$ state (because associated the Clebsch-Gordan coefficientn is zero). We therefore have one non-coupled state no matter what the polarization of the field is for an $F \to F' = F$ transition. A similar reasoning (figure 3(a) (down)) shows that for an $F \to F' = F - 1$ there are two non-coupled states.

This simple picture needs to be generalized once we have more than one beam and each with different polarizations. The interference of beams with different polarizations leads to a total electric

† The usual role of the repumper beam is to recycle the atoms that decay spontaneously to the ground state we are not aiming at with our laser.

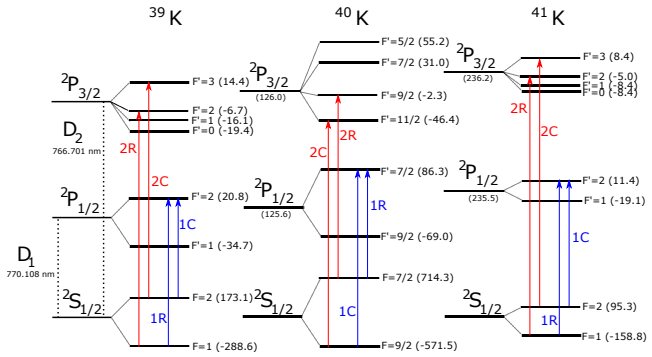

Figure 2. Fine and hyperfine structure of the three isotopes of potassium. In parenthesis we show (in MHz) the energy shifts of the both fine states from ^{4}0K and ^{4}1K with respect to those of ^{3}9K, and also the energy difference between each hyperfine state with respect to the energy of the fine state to which they correspond. We also show the cooling and repumping transitions used. In the experiment, the transitions for the D_2-line will be red detuned and the ones corresponding to the D_1-line will be blue detuned. Frequencies taken from [11].

field that might present a spatial gradient of polarization. The non-coupled state will be, in this case, a linear combination of the Zeeman substates of the ground state manifold. And the same for the coupled state(s). Moreover, the coupled state energy will be also modulated in space due to the fact that the coupling of the atomic dipole operator with the electric field is itself polarization dependant. As we will see, this energy modulation is (in a similar fashion as Sisyphus cooling) another key point of the cooling mechanism. The light sfhits are proportional to the detuning, and for a blue detuned beam the modulated energies are positive and above the energy of the non-coupled state.

We have been specially careful calling the non-coupled state *non-coupled* and not *dark* state This is due to the fact that the non coupled state is not necessarily an eigenstate of the kinetic energy operator. It is therefore possible for the atoms to escape from this non-coupled state if they have certain velocity, due to motional coupling (hence the name *gray* molasses). Therefore, an atom starting at the point $\mathcal{M}$ in figure 3(b) has a certain probability (proportional to v^2 and bigger at the energy minima of the coupled state) of being transfered to the coupled state (point $\mathcal{N}$), there, after losing kinetic energy from $\mathcal{N} \rightarrow P$ due to the potential hill (as in Sisyphus cooling), can be optically pumped back to the non-coupled state$\mathcal{Q}$. This cycle is repeated until the probability of departure from the non-coupled state is negligible.

3.3. Gray Molasses in our system

The discussion presented above applies also to our $F = 2 \rightarrow F' = 2$ transiton. However, the real situation involves other points that need to be taken into account. First of all, we are not in 1D but in 3D, which means that the beams interacting will involve terms containing different polarization gradients. Moreover, we are also using a repumper, so another ground state hyperfine manifold needs to be taken into account in the discussion. We are dealing with a Λ-system and when the Raman condition is satisfied this can also lead to a cooling enhancement (known as Λ-enhanced cooling in gray molasses [13, 14]) due to the appearance of additional dark states.

4. The D_1-line laser system

The laser system used to perform the cooling previously described is sketched in figure 4. It is designed so that it can deliver the necessary frequencies to act on the three isotopes, which is

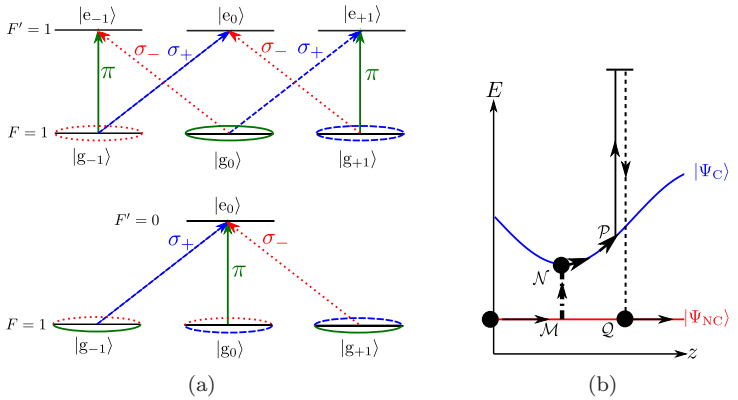

(a) (b)

Figure 3. (a) Non-coupled states for different transitions. (up) - $F = 1 \rightarrow F' = 1$ transition . (down) - $F = 1 \rightarrow F' = 0$ transition. The circles show for which polarisation the state is not coupled. (b) Sisyphus cycle undergone by an atom. On average, the light field wins energy and therefore the atoms are slowed down after an $\mathcal{MNPQ}$ cycle.

achieved by means of acusto-optical modulators (AOMs). The repumping beam is created by means of electro-optical modulators (EOMs). To make sure that the frequency is stable, saturated absorption spectroscopy is performed in order to lock the laser. Finally, in order to obtain a high intensity beam a tapered amplifier † is used and the light is coupled into an optical fiber that is part of a 4 to 4 fiber cluster ‡

4.1. Frequency locking

In order to obtain a light source stable in frequency we need to lock our laser, a Toptica DL pro external cavity diode laser.

By means of a piezoelectric actuator it is possible to change the angle of a grating profile, which changes the lasing frequency. This frequency can also by tuned by changing the temperature and/or the current.

The desired frequencies are the ones shown in the figure 2, and we will blue detune our laser with respect to these transitions by $\Delta = 3\Gamma$.

To lock our laser, we will stabilize it in one of the frequencies ^{39}K. We do this because we are working with a non-enriched cell containing potassium and the abundancies of the isotopes are 93.2581(44)%, 0.0117(1) and 6.7302(44)%, respectively for ^{39}K, ^{40}K and ^{41}K, [11]. Therefore we will only be able to record the absorptiom spectrum of ^{39}K.

The technique used to obtain the resonances is known as saturated absorption spectroscopy, and we will use the frequency modulation (FM) spectroscopy technique in order to generate the error signal that will allow us to lock the laser in one of these resonances.

4.1.1. Saturated absorption spectroscopy

It consists in retroreflecting a beam through a cell containing potassium vapour and recording the output while scanning the external cavity of the laser. With this technique, we are able to superimpose the real transitions occurring to the gaussian absorption profile due to Doppler broadening that appears when we send non-resonant beams.

† Eagleyard Photonics Tapered Amplifier EYP-TPA-0765-01500-3006-CMT0. This semiconductor device is driven at 2.5 A and stabilised in temperature by means of a PID-Controller.
‡ Evanescent Optics Fiber cluster: 4x4 Splice-less PM Coupler Array.

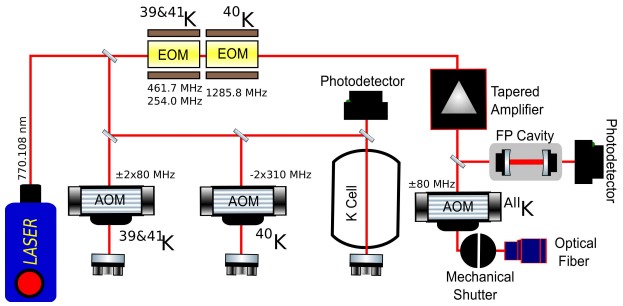

Figure 4. Scheme with the main elements of the laser system for the D_1-line cooling.

To see why this is possible, let's consider an atom at rest (i.e. seeing both beams at the same frequency). In this case, for zero detuning for a determinate hyperfine resonance, the beam we send (pump) is absorbed by the atoms at rest and saturates the transition. After this, some of the excited atoms will spontaneously decay to another ground state. As a result, the retroreflected beam (probe) has less atoms to excite and will be less absorbed, resulting in more photons reaching the photodetector. This tourns out in a lorentzian peak in the gaussian profile (i.e. we are able to detect the real transition).

We observe two more kind of transitions corresponding to another velocity class (see figure 5(b)): for $v = \pm(\omega_1 + \omega_2)/2k$ we can either have crossover transitions or 4-level resonances. We therefore have 9 possible transitions (because the two 4-level resonances lead to the same laser frequency) in which we can lock our laser.

We have chosen, for stabilisation, the crossover ransition between $F = 1 \rightarrow F' = 2$ and $F = 2 \rightarrow F' = 2$. The energy shifts with respect to the cooling transitions in the D_1-line at detuning $\Delta = 3\Gamma$ from figure 2 are shown in table 1. We will show in Sec. 4.2.1 how to perform these shifts.

4.1.2. FM Spectroscopy

As we said, by changing the amplitude and the offset of the piezoelectric actuator, we can control the frequency of the laser so that it goes to any of the spectroscopic features. We want now this frequency to be stable. For this, we generate an error signal that tells us wheter this frequency is either drifting to higher values or smaller values of the resonance. This cannot be directly known from the intensity recorded in the spectroscopy, but it can from its derivative (the maximum of intensity will correspond to a zero in its derivative). For this we use FM-Spectroscopy. What we do is modulate in frequency the laser by creating sidebands of the order of $5 - 20$ MHz. It can be shown [15] that if 1) we shine this light to a photodiode (fast enough to record the modulation) after the cell, 2) we filter the high frequency components, 3) we now multiply this signal with the source generating the modulation (downmixing) and 4) filter out the components with a frequency higher than the modulation one, we obtain a signal that is proportional to the derivative of the spectroscopy§. Now, with a PI-Controller that controls both the piezoelectric crystal and the intensity that arrives to the laser, we are able to lock the laser to the desired frequency.

§ We use a Thorlabs PDA10A-EC photodetector a RIGOL DG-1000 Series Dual Channel Function arbitrary wave form generator and the following MiniCircuits components: ZEDC-15-2B coupler, ZX05-1MHW-S+ frequency mixer, SLP-2.5+ low pass filter, ZFL-500LN+ amplifier, BLK-89-S+ DC block and ZFBT-4R2GW bias-tee.

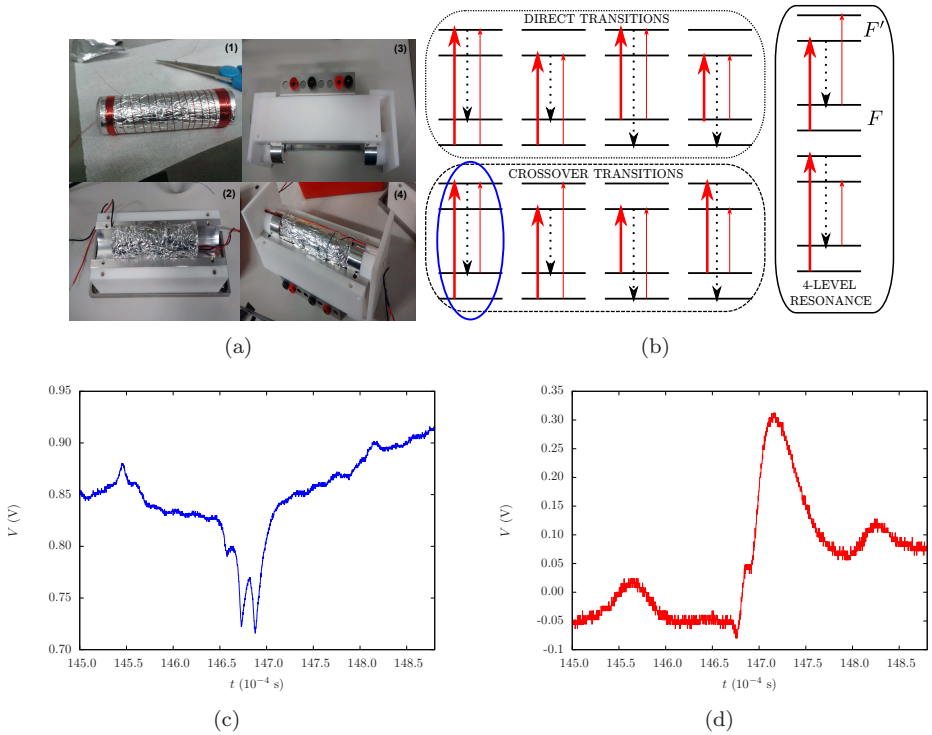

Figure 5. (a) Construction steps of the potassium heating cell. (1) Cell and bifilar element wound. (2), (3) and (4) show different perspectives of the sourrounding heating element. (b) Possible transitions in saturated absorption spectroscopy for ^{39}K. The crossover transition between $F = 1 \rightarrow F' = 2$ and $F = 2 \rightarrow F' = 2$ chosen for stabilisation is marked with a blue circle. The thick arrow corresponds to the pump beam, the thin one to the probe and the dashed one indicates spontaneous emission. (c) Recorded saturated absorption spectroscopy. The crossover chosen corresponds to the deepest peak in the right. (d) Error signal corresponding to the spectroscopy shown in (c).

4.2. Procedures followed to set the laser system

In this section we will detail the construction of some the laser system parts: the selection of the right frequencies for the cooling beam, the potassium heating cell for the saturated absorption spectroscopy, the setting up of the drivers for the EOMs that generate the repumper sidebands and the design of a confocal Fabry-Perot cavity.

4.2.1. Selection of the cooling frequencies

Since we have locked our laser at a frequency that is not ours, we need to shift it to the correct transition. This is done by mean of the AOMs from figure 4: two of them (the ones in the same part of the spectroscopy) are in a double pass configuration, and the other one (after the TA) shifts it only once. The reason why we choose that crossover is double: it is the biggest feature in the spectroscopy (deepest peak from figure 5(c)), and by locking in this transition, we can do the shifts with the minimum number of standard AOMs‖.

After the double-pass AOMs ¶ the frequency is shifted to $\omega_L \rightarrow \omega_L + 2\Omega$, where ω_L is the frequency of the laser light and Ω the shift added by the AOM.

‖ We use 80 MHz ATM-801A2 and 310 MHz ATM 30101A2.12 AOMs from Intraaction.
¶ It consists of an AOM + $\lambda/4$ waveplate +lens in cat-eye configuration + retro-reflecting mirror. After the second pass, the chosen order is aligned with the optical aixs.

Isotope	$\Delta\nu_{\text{before}}$ (MHz)	Ω (MHz)	Ω' (MHz)
^{39}K	-212.76	+66.38	-80
^{40}K	722.94	-321.47	+80
^{41}K	91.14	-85.87	-80

Table 1. Frequency shifts for all the isotopes before and after the AOMs and frequencies of the AOMs employed.

Therefore, now we have that $\omega_{\text{L}} + 2\Omega = \omega_{\text{c}}$, where ω_{c} is the frequency of the crossover in which we stabilize the laser.

In the other part of the laser system, we have another AOM (that is also used to change the direction of the beam when we don't want light coupled into the fibre) that adds another shift Ω'. Therefore: $\omega_{\text{L}} = \omega_{\text{c}} - 2\Omega + \Omega'$.

Finally, we want that ω_{L} be the frequency of the resonant transition of the isotope we're dealing with. The best combination of AOMs we found for this is the one shown in table 1.

4.2.2. Construction of the potassium heating cell

In order to observe the spectroscopy we need to retroreflect the beam through a cell containing potassium vapour. Due to its low vapour pressure (compared to Rb, for instance) of $1,3 \times 10^{-8}$ mbar at room temperature [11], we need to heat up the cell. For this, we wound a bifilar heating element (to avoid magnetic fields) around the glass cell. We used a wire of $\varnothing = 0.1$ mm and $L = 20$ m. We had two main problems: the first one is that potassium condensed on the windows of the cell (which were colder), this was solved by coiling more wire in the extremes than in the center. The other is that there were fluctuations in the spectroscopy, we believe due to air turbulence. It was solved by filling the free space between the end of the cell and its support with a cylindric aluminum piece with a whole in the middle (which also helped to heat more the windows). The cell was supported by aluminum surrounded by teflon to isolate it thermally from the table. So far, the best parameters in order to observe a good spectroscopy are to use a current of $I = 1.5$ A at 16.0 V, which puts the cell at approximately 110 °C, for which we obtain a 31% of absorption.

4.2.3. Construction of a Confocal Fabry-Perot cavity

In order to control the intensity between the repumper beam and the cooling beam, to check that the frequencies of the sidebands were the ones we expected and that the laser is not multimode, we also built a confocal Fabry-Perot cavity. A confocal resonator consists of two spherical mirrors whose radii $R_1 = R_2 \equiv R$ are equal to the length of the cavity L.

For a Gaussian beam, the frequency spectrum is given by: $\nu_{qmn} = c\left[2q + (m + n + 1)\right]/4L$, where L is the length of the cavity, q designs the longitudinal modes and m, n the transverse modes. We can see that all modes for which $2q + m + n$ is equal will have the same frequency despite the fact that they lead to different spatial configurations. The fact that the transverse modes are degenerated at the longitudinal mode frequency, presents the advantadge that the cavity doesn't need to be perfectly aligned nor mode matched. So, even though we will probably be exciting a many higher order modes, we will also be exciting the fundamental one. Therefore, despite the fact that longitudinal modes are still are separated by $c/2L$, the degenerancy makes that even-symetry modes of the cavity are degenerated at the longitudinal mode frequency and the odd-symetry ones at half of it. Consequently, the free spectral range of such a cavity is $c/4L$ [16].

For our cavity, given the distances between hyperfine states of the ground state manifold, we have chosen the length of the cavity to be $L = 10$ cm and so are the radii of the mirrors. We

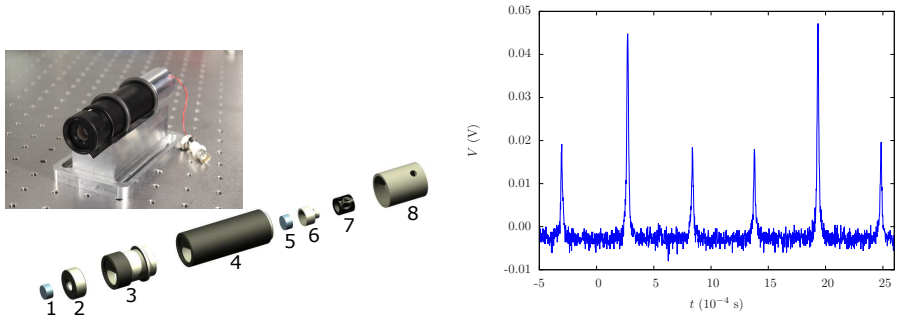

(a) (b)

Figure 6. (a) (up) - Cavity in its mount. (Down) - (1) and (5) mirrors (2) SM1A6T-Thorlabs adapter (3) SM1V10-Thorlabs adjustable tube, allows to adjust coarsely the length of the cavity (4) SM1L30-Thorlabs tube (6) mirror support (7) piezoelectric stack and (8) suport for the piezoelectric stack. (b)Recorded spectrum of the confocal Fabry-Perot cavity. We see the cooling beam and the repumper beam sidebands at 254.0 MHz.

have done this because it gives a free spectral range $\Delta\nu = 750$ MHz, which means that none of our rempumper frequencies will be at the end of a scanning. The reflectivity of the mirrors[+] is $\mathcal{R} = 0.988$, its calculated finesse is $F \sim 131$ and the full width at half maximum FWHM $\sim$ 5.7 MHz (on the order of the transition linewidth). The components of the cavity are shown in figure 6(a) (where we can also see the cavity and its support). In order to scan the cavity, we use a low voltage piezoelectric stack [*] (7) mounted to one of the mirrors (5). Most of the pieces are comercial mounting elements except from (6) and (8), that are custom-designed. In a second version of the cavity, (6) was substituted by a comercial support screwed to the piezo in which the mirror can be fixed, which improved the alignment of the cavity (since probably the mirrors are less tilted). The piezoelectric stack is connected by means of a BNC cable to a wave function generator[♯] in order to scan the cavity.

In figure 6(b) we show the spectrum of the cavity with the EOM for ^{41}K connected (i.e. creating the repumping sidebands at 254 MHz from the cooling beam).

4.2.4. EOM drivers

In order to generate the repumper frequencies ($\nu_{39} = 461.7$ MHz, $\nu_{40} = 1285.8$ MHz and $\nu_{41} = 254.0$ MHz) we use two different EOMs that will create the sidebands in the cooling beam. One of these has a crystal that can be resonant to the frequencies needed both ^{39}K and ^{41}K, and the other one is resonant to ^{40}K. The radiofrequencies needed are generated by Voltage Controlled Oscillators (VCOs) and their power is controlled by means of Voltage Controlled Atenuators (VCAs). This frequency is then sent to an amplifier than finally sends it to the EOM. In order to use the same amplifier for the bosonic isotopes, a switch controlled by an external TTL is added before the amplifier. We built an electronic circuit that, by means of voltage regulators (LM7805 and LM317) and potentiometers allows to control all the electronic components (except the amplifiers) from the same 15V power supply and obtain the right frequencies and intensity ratios [††] .

[+] Layertec GmbH 107880 mirrors. Dimensions: ⌀12,7×6,35 mm.
[*] Piezomechanik low voltage piezoelectric ring actuator without casing, stack tipe, PHPSt 150/14-10/12.
[♯] GwINSTEK Synthesized function generator. SFG-1000 Series.
[††] Minicircuits components: VCOs: ZOS-535+, ZX95-1420-S+ and ZOS-400+. VCAs: X73-2500-S+, ZX73-2500-S+ and ZX73-2500-S+. Amplifiers: ZHL-1-2W-S+, ZHL-1217HLN and ZHL-1-2W-S+. Switch: ZASW-2-50DR+.

5. Conclusions

During this project a laser system to implement gray molasses sub-Doppler cooling in the D_1-line of potassium gases has been designed and constructed. In order to accomplish it, besides the assembly and alignement of the elements itself, several sub-projects have been performed, including:

- For the frequency stabilization of the laser: the choice of a frequency in which stabilize, the building of a mechanism to heat the cell, the AOMs needed to obtain the shift to the desired frequencies, and the lock itself.
- For the power amplification: from an existing mount design original from our grup, a tapered amplifier has been mounted there an optimized. Its protection circuit has been welded and a PID-controller for the temperature has been set.
- For the repumper frequencies: the calculation of the powers needed for each EOM, the assembly of all the RF needed for them to work and the design and construction of the electronic circuit to control the RF source.
- The design and construction of two confocal Fabry-Perot cavities.
- Small participation in the assembly of the vacuum system and other parts of the laser system.

The optical bench and the corresponding electronics are now fully operational and integrated on the experimental setup.

The actual state of the experiment is the following: the whole laser system, the magnetic field coils, the RF sources for evaporative cooling and the computer control system are completely finished. The vacuum system is also close to completion, which means that the gray molasses scheme built during this thesis will be tried on the atoms in the following months.

Acknowledgments

I want to express my gratitude to Leticia Tarruell for giving me the opportunity to participate in the setting up of the experiment and her advise. I also want to thank Pierrick Cheiney, César Cabrera, Vincent Lienhard and Jordi Sastre for the good moments and their constant help. Isabel Fernández is also acknowledged for her useful comments.

References

[1] Bloch I, Dalibard J and Nascimbène S 2012 *Nat. Phys.* **8**, 267-276
[2] Greiner M, Fölling S 2008 *Nature* **453**, 736-738
[3] Bloch I, Dalibard J and Zwerger W 2008 *Rev. Mod. Phys.* **80**, 885-964
[4] Boiron D, Trich C, Meacher D.R, Verkek P and Grynberg G 1995 *Phys. Rev. A* **52**, R3425
[5] Rio Fernandes D, Sievers F, Kretzschmar N, Wu S, Salomon C and Chevy F 2012 *EPL*, **100** 63001
[6] Salomon G, Fouché L, Wang P, Aspect A, Bouyer P and Bourdel T 2013 *EPL* **104** 63002
[7] Metcalf H.J and van der Straten P 1999 *Laser Cooling and Trapping*(Springer-Verlag, New York)
[8] Chaudhuri S, Roy S, Unnikrishnan C.S 2006 *Phis. Rev. A* **74** 023406
[9] Dalibard J and Cohen-Tannoudji C 1989 *J.O.S.A.* **B** 6, 2023
[10] Lin Y.J, Perry A.R, Compton R.L, Spielman I.B and Porto J.V 2009 *Phys. Rev. A* **79**, 063631
[11] Tiecke T.G 2010 *Properties of Potassium.* http://staff.science.uva.nl/~tgtiecke/PotassiumProperties.pdf
[12] Cohen-Tannoudji C 1995-1996, *Cours du Collège de France* 1995-1996
[13] Grier A.T, Ferrier-Barbut I, Rem B.S, Delehaye M, Khaykovich L, Chevy F and Salomon C 2013 *Phys. Rev. A* **87** 063411
[14] Nath D, Kollengode Easwaran R, Rajalakshmi G, Unnikrishnan C S 2013 *Phys. Rev. A* **88**, 053407
[15] Bjorklund G.C 1980 *Optics Letters* **5**, 1, 15-17
[16] Siegman A.E, 1986 *Lasers* (California, University Science Books)